PHOTOCONDUCTIVITY

The term *photoconductivity* refers to phenomena involving a change in the electrical conductivity of a material as a result of the excitation of new free charge carriers through the absorption of light (1). It is highly sensitive to the presence of defects or impurities in a material, as well as to the crystalline structure of the material. Photoconductivity is also a member of a larger category of phenomena such as changes in electrical conductivity caused by irradiation with X rays or high-energy electrons. The adjectives used to describe phenomena falling into this general category have included photoelectric, photoelectronic, optoelectronic, and photonic.

Photoconductivity can be useful as the means by which the presence and intensity of various kinds of radiation are measured, in applications in which the photoconductor plays the role of a circuit element with a resistance that is radiation dependent, and as a research effect useful in detecting and characterizing defects and impurities in the material. Other related phenomena are photoexcitation-caused changes in the Hall effect (photo-Hall effect), the thermoelectric effect (pho-

tothermoelectric effect), and the capacitance of a semiconductor junction (photocapacitance). In all of these applications, an external voltage is applied to the material in which photoconductivity and related effects are important. When additional charge carriers are photoexcited in a material containing an internal electric field, a current and voltage are generated even in the absence of an applied external voltage (photovoltaic effect).

BASIC PHOTOCONDUCTIVITY PROCESSES

A general diagram for the main phenomena involved is given in Fig. 1 for a typical semiconductor. This is an energy-band diagram (a plot of electron energy versus position) in which electrons in extended conduction states (the conduction band) are separated from electrons or holes (missing electrons) in valence states (the valence band) by the band gap, in which only localized energy states associated with crystal imperfections such as crystal defects or impurities exist. The major processes of interest are optical absorption by which free carriers are created, electrical transport by which free carriers contribute to the electrical conductivity, capture of free carriers leading to recombination, and thermal excitation of trapped carriers to the nearest band.

Optical absorption resulting in an increase in free carriers may be the result of an intrinsic photoexcitation process from the valence band to the conduction band of a semiconductor [Fig. 1(a)], in which case equal densities of electrons and holes are initially produced. It may also result from an extrinsic photoexcitation process from electron-occupied imperfection states to the conduction band [Fig. 1(b)], in which case only free electrons are produced, or from the valence band to electron-unoccupied imperfection states [Fig. 1(c)], in which case only free holes are produced. Such optical absorption is described quantitatively through the absorption constant α. In the simplest case, neglecting effects due to reflection or interference, if light with intensity I_0 is incident on a sample with thickness d and absorption constant α, the transmitted light intensity is expressed by a relationship known as Beer's law,

$$I = I_0 \exp(-\alpha d) \tag{1}$$

The magnitude of α for intrinsic photoabsorption can be calculated by a quantum-mechanical perturbation calculation in which the effect of the light is treated as a perturbation in the basic Schrödinger equation. In the case of extrinsic photoabsorption α can be simply expressed as $\alpha = S_{opt}N$, where N is the density of imperfections involved in the absorption process, and S_{opt} is a quantity called their optical absorption cross section (usually of the order of 10^{-16} cm^2).

Free electrons may be captured by unoccupied imperfections [Fig. 1(d)], or free holes may be captured by electron-occupied imperfections [Fig. 1(e)]. This capture process is described through a capture coefficient β such that the rate of capture R of free carriers with density n by defects with density N is given by $R = \beta nN$. The magnitude of β depends on the details of the capture process, that is, on the mechanism by which the energy of the recombining carrier is dissipated, and on whether the imperfection is electrically neutral, charged the same as the carrier being captured, or opposite to the charge of this carrier. A energy-dependent capture cross section $S(E)$ is often defined such that $\beta = \langle S(E)v(E)\rangle = Sv$, where the average is over electron energy, S defined by this relation is called the capture cross section, and v is the average thermal velocity of a free carrier.

In the case of one-carrier effects, assuming electrons to be the dominant carriers, the lifetime of a photoexcited electron, τ_n, that is, the average time the photoexcited electron is free before recombination, is given by $\tau_n = 1/\beta_n N$ when imperfection recombination dominates. Since the rate of capture, or in this case the rate of recombination R (per unit volume per second), is equal to $\Delta n/\tau$, where Δn is the increase in electron density due to photoexcitation, and in steady state the rate of recombination must be equal to the rate of photoexcitation G (per unit volume per second), the result is the basic steady-state relationship fundamental to all photoelectronic phenomena,

$$\Delta n = G\,\tau_n \tag{2}$$

In many practical applications of photoconductivity, $\Delta n \gg n_0$, where n_0 is the dark (equilibrium) free-electron density, and the total observed electron density under photoexcitation can be taken to be essentially equal to Δn.

When a photoexcited free electron is captured at an imperfection, it may subsequently recombine with a free hole, or it may be thermally reexcited to the nearest band before recombination can occur. In the latter case, the imperfection is referred to as an electron trap; Fig. 1(f) shows examples of both capture (trapping) and thermal reexcitation (detrapping) of an electron at a shallow electron trap, and of both capture and thermal reexcitation of a hole at a shallow hole trap. The behavior of a specific imperfection may change from that of a recombination center to that of a trap with changes in photoexcitation intensity and/or temperature.

Two other important aspects of the discussion of photoconductivity are shown in Fig. 1: the contacts to the material and the transport processes of free carriers in the material. Contacts may be *ohmic,* in which case they allow the free flow of free carriers into and out of the material required to maintain charge neutrality; *blocking,* in which case the contacts

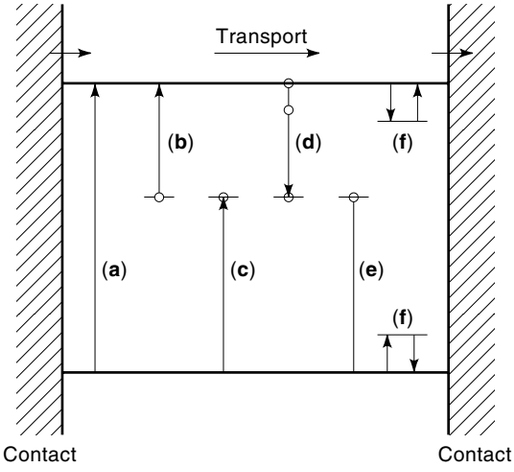

Figure 1. Major transitions and phenomena associated with photoelectronic effects in homogeneous semiconductors: (a) intrinsic absorption, (b) and (c) extrinsic absorption, (d) and (e) capture and recombination, (f) trapping and detrapping. Arrows indicate electron transitions.

form depletion layers in the material adjacent to the contacts and are unable to supply the carriers needed to maintain charge neutrality when carriers move out of the material due to the imposed electric field; or *injecting,* in which case the contacts actually inject carriers into the material at a rate greater than their departure rate at the other contact, thus causing a space charge in the material.

The specific contribution of the photoexcited carriers to the electrical conductivity of the material depends on the nature of the active transport processes. The electron *drift* current J_{drn}, for example, depends on the electrical conductivity σ_n and the electric field $\mathscr{E}$, $J_{drn} = \sigma_n \mathscr{E}$. The electrical conductivity depends on the density of free electrons and their mobility μ_n: $\sigma_n = nq\mu_n$, where q is the electronic charge. The electron mobility is the ratio of the electron velocity (due to the electric field) and the magnitude of the electric field present ($v_n = \mu_n \mathscr{E}$), and can be expressed as $\mu_n = (q/m_n^*)\tau_{sc}$, where m_n^* is the electron effective mass and τ_{sc} is the average time between electron scattering events, called the scattering relaxation time. The electron *diffusion* current results when there is a gradient in electron density ∇n, and $J_{dfn} = qD_n \nabla n$, where the electron diffusion coefficient $D_n = \mu_n kT/q$. The total current is the sum of drift and diffusion currents.

PHOTOCONDUCTIVITY PARAMETERS

Descriptions of photoconductivity focus on three basic aspects of the phenomenon: the photosensitivity, the spectral response, and the speed of response. As background, we first consider the nature of fundamental photoconductivity processes.

In the most general case of a semiconductor with both free electrons and free holes, the electrical conductivity in the dark is given by $\sigma_0 = q(n_0\mu_{n0} + p_0\mu_{p0})$. Under photoexcitation, this conductivity is increased to σ_L, the conductivity in the light, and the photoconductivity itself is defined as $\Delta\sigma$ such that

$$\sigma_L = \sigma_0 + \Delta\sigma \tag{3}$$

In the case in which only electrons are the free carriers, for example,

$$\sigma_0 + \Delta\sigma = (n_0 + \Delta n)q(\mu_0 + \Delta\mu) \tag{4}$$

where we recognize that the change in conductivity with light may also be due to a change in mobility as well as a change in electron density. Then

$$\Delta\sigma = q\mu_0\Delta n + (n_0 + \Delta n)q\Delta\mu \tag{5}$$

Since it is generally true that $\Delta n = G\tau_n$ [Eq. (2)], it follows that

$$\Delta\sigma = q\mu_0 G\tau_n + nq\Delta\mu \tag{6}$$

When account is taken of the fact that the lifetime τ_n itself may also be a function of photoexcitation intensity, three types of effects are possible in determining the quantities in Eq. (6).

1. An increase in carrier density with constant lifetime, as is the case when capture of photoexcited carriers occurs through imperfections the occupancy of which is not materially affected by the recombination process itself. In this case,
$$\Delta\sigma = q\mu_0\tau_n G \tag{7}$$
2. An increase in carrier density with an excitation-dependent lifetime, $\tau_n \propto G^{(\gamma-1)}$ so that $\Delta\sigma$ varies as G^γ. If the capture probability by imperfections increases with photoexcitation intensity as the density of imperfections involved in recombination increases, the lifetime decreases with increasing excitation rate, $\gamma < 1$, and the behavior is said to be *sublinear.* If the capture probability by imperfections decreases with photoexcitation intensity, as when recombination shifts from imperfections with large capture cross sections to those with smaller capture cross sections, the lifetime increases with increasing excitation rate, $\gamma > 1$, and the behavior is said to be *superlinear.*
3. An increase in carrier mobility, so that $\Delta\sigma = nq\Delta\mu$. Although frequently a minor effect, such a $\Delta\mu$ can result from (a) a decrease in scattering by charged imperfections as photoexcitation removes the charge on some of these imperfections, (b) a reduction in the barrier height and the depletion width in the adjacent grains because of the photoexcited increase in free-carrier density, if the material is polycrystalline and contains intergrain potential barriers that limit the effective mobility, or (c) photoexcitation that takes a free carrier from a band with one mobility to a higher band with a larger mobility.

Photosensitivity

The critical parameters for the sensitivity of the photoconductivity process, that is, the magnitude of $\Delta\sigma$ for a specified photoexcitation rate, are given from Eq. (7) as

$$\Delta\sigma/Gq = \tau_n\mu_n \tag{8}$$

Thus the lifetime–mobility product gives a figure of merit for the photoconductor's sensitivity to light.

Another often-used definition of photosensitivity is *photoconductivity gain.* The gain of a photoconductor is defined as the number of charges collected in the external circuit for each photon absorbed. The conditions that give rise to gains greater than unity are discussed in the treatment of different typical photoconducting systems below. The connection between these two definitions can be seen by considering F as the total number of photons absorbed per second, so that the photoexcitation rate $G = F/Ad$, and the gain G^* can be expressed

$$G^* = (\Delta I/q)/F = \tau_n\mu_n V/d^2 \tag{9}$$

using $\Delta I = \Delta\sigma AV/d$, $\Delta\sigma = \Delta nq\mu_n$, and $\Delta n = G\tau_n$.

The concept of photoconductivity gain can also be seen to be equivalent to saying that the gain of a photoconductor is equal to the ratio of the carrier lifetime to the carrier transit time ($d/[\mu_n(V/d)]$) through the material, that is, $G^* = \tau_n/(d^2/\mu_n V)$. Thus if the lifetime of a carrier is greater than its transit time, it will make several effective transits during its lifetime through the material between the contacts, provided that the contacts are ohmic and able to replenish carriers drawn off at the opposite contact.

Spectral Response

Since light must be absorbed by the material in order to produce photoconductivity, a strong correlation is expected between the absorption spectrum and the spectral response of photoconductivity. Figure 2 compares typical experimental spectral response curves for photoconductivity [Fig. 2(a)] for the applied electric field normal to the direction of photoexcitation and relates three main regions in the absorption spectrum with the shape of the spectral response of photoconductivity [Fig. 2(b)]. The three principal regions indicated are region I, controlled by the surface lifetime in the high-absorption region, usually smaller than the bulk lifetime because of a higher density of surface imperfections; region II, controlled by the bulk lifetime with a maximum occurring when the absorption constant is approximately equal to the reciprocal of the sample thickness; and region III, still controlled by bulk lifetime but with absorption decreasing with increasing wavelength.

Speed of Response: Effect of Traps

The speed of response of a photoconductor is a measure of how rapidly it can respond to changes in photoexcitation intensity. The rise time is the time required for the increase of photoconductivity to $1 - 1/e$ of its steady- state value after being turned on, and the decay time is the time constant associated with the decrease of photoconductivity to $1/e$ of its photoexcited steady-state value after the photoexcitation is turned off.

One of the major effects of trapping phenomena involving the time-dependent phenomena of trap filling and emptying is to decrease the speed of response to changes in photoexcitation intensity. In the absence of traps, the time constant associated with the rise and decay of photocurrent is given simply by the lifetime of the free carriers involved. A simple description of the decay response time τ_0 in terms of the lifetime τ_n can be given by

$$\tau_0 = \tau_n(1 + n_t/\Delta n) \tag{10}$$

where n_t is the density of traps that must empty in order for the steady-state Fermi energy to drop by kT (corresponding to the requirement that the photoconductivity decrease during decay by $1/e$ in a time τ_0). If $\Delta n \gg n_t$, as for low trap densities and/or high photoexcitation intensities, $\tau_0 = \tau_n$. But if $\Delta n \ll n_t$, as for high trap densities and/or low photoexcitation intensities, $\tau_0 = \tau_n(n_t/\Delta n)$.

Traps also have two other significant effects on overall photoconductivity performance. (1) They cause the effective drift mobility to decrease. The drift mobility is determined by the time t_{dr} it takes carriers injected at one point in the sample to travel to a second point distant from it by d under an electric field $\mathscr{E}$: $\mu_d = d/\mathscr{E}t_{dr}$. If there are no traps, an injected carrier moves with the normal conductivity mobility, but when traps are present an injected carrier spends a major part of its time in traps and only a small fraction of that time is it free and able to move. This effect is simply described by the following relation between the drift mobility and the conductivity mobility: $(\Delta n + n_t)\mu_{dr} = \Delta n\mu$, which is similar to Eq. (10) for the response time versus lifetime relationships for $n_t \gg \Delta n$. (2) Traps can also cause the photosensitivity to decrease. Let N_r^* be the density of imperfection recombination sites facing a free electron. In the absence of traps a photoexcited electron in the conduction band corresponds to either a localized hole at an imperfection or a free hole in the valence band, that is, $\Delta n = N_r^* + \Delta p$, with the expectation that $N_r^* \gg \Delta p$ normally and therefore $N_r^* \approx \Delta n$. But in the presence of traps, many of the photoexcited electrons have been trapped and now $N_r^* = \Delta n + N_t \approx N_t \gg \Delta n$. Thus the lifetime has been reduced by the factor $\Delta n/N_t$.

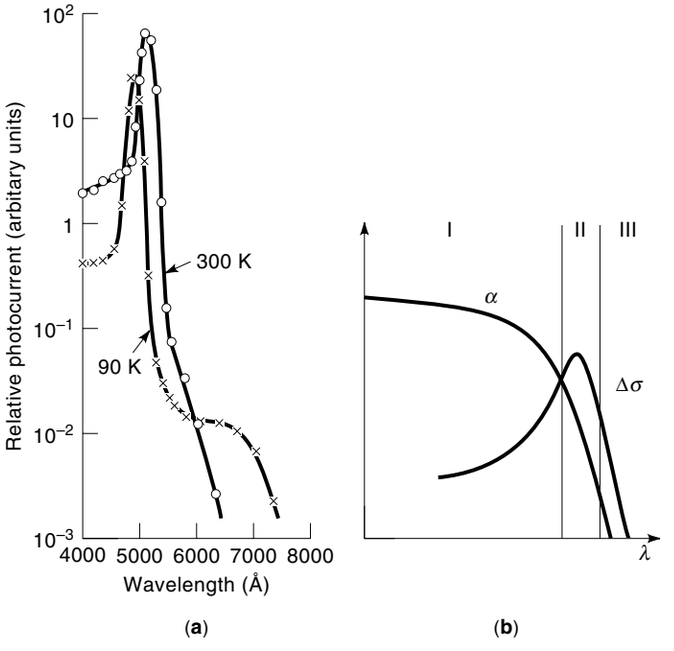

Figure 2. (a) Photoconductivity spectral response curves for a crystal of CdS at 90 K and 300 K, showing the effect of the shift in the optical absorption edge to longer wavelengths at higher temperatures. (b) Comparison of the photoconductivity spectral response and the absorption constant of the material, defining three characteristic regions.

TYPES OF PHOTOCONDUCTING SYSTEMS

The different types of photoconducting systems can be conveniently separated into two main types: homogeneous and semiconductor junction.

Homogeneous Material

Figure 3 shows five different possibilities for photoconducting behavior in a homogeneous material, depending on the behavior of the contacts, and the importance of photoexcited carrier capture at imperfections.

Figure 3(a) corresponds to a material with ohmic contacts for both electrons and holes and without any imperfections. Photoexcitation produces free electrons and free holes that move through the material, being replaced at one contact when they leave the material at the other, until they recombine with one another. The gain is simply the sum of the electron gain and the hole gain, $G^* = (\tau_n\mu_n + \tau_p\mu_p)V/d^2$. This is an ideal case not normally encountered with real materials.

Figure 3(b) is the same as Fig. 3(a) except that the contact for hole replacement is not ohmic. This means that the effec-

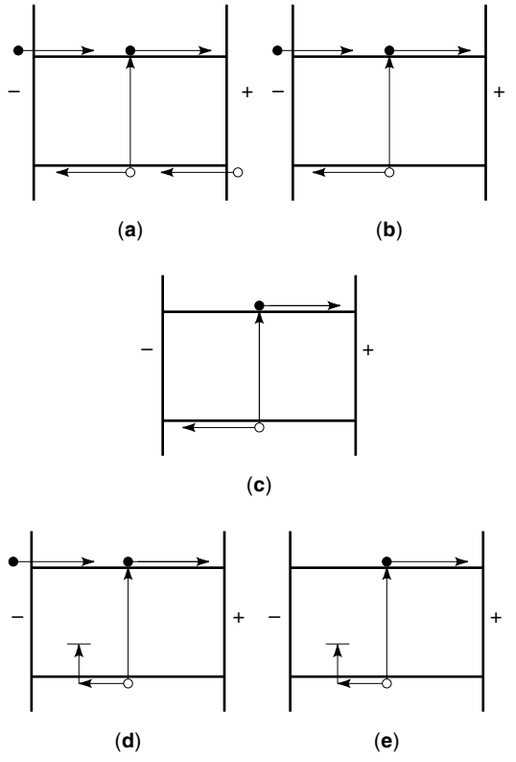

Figure 3. Five basic types of homogeneous photoconductor.

tive hole lifetime is the hole transit time and that the effective electron lifetime, during which electrons will be replaced by the ohmic contact for electrons, is also the hole transit time. The gain is given by $G^* = (1 + \mu_n/\mu_p)$.

Figure 3(c) is the same as Fig. 3(a) except that neither contact is ohmic. The lifetimes for electrons and holes are both equal to their corresponding transit times, and the gain is simply unity. Cases for which $G^* = 1$ have historically been referred to as *primary photoconductivity.*

Figure 3(d) introduces the possibility of capture of the photoexcited hole at an imperfection, with the electron contributing to the conductivity, with successive replacement at the electron-injecting contact, until it recombines with the captured hole. The gain is due to the electron conductivity and is given by Eq. (9). This is the "normal" situation in a sensitive homogeneous photoconductor, showing gains greater than unity. Cases for which $G^* > 1$ have historically been referred to as *secondary photoconductivity.*

Figure 3(e) corresponds to the same case as Fig. 3(d), except that neither contact is ohmic. The photoexcited hole is captured at an imperfection, the material polarizes, the trapped charge cancels the applied field, and no steady photoconductivity can flow.

Semiconductor Junctions

Perhaps the simplest type of semiconductor junction is provided by a blocking contact such as that just referred to. Such a blocking contact, called a *Schottky barrier,* is obtained on an *n*-type material by using a metal with a work function larger than that of the semiconductor and on a *p*-type material by using a metal with a work function smaller than that

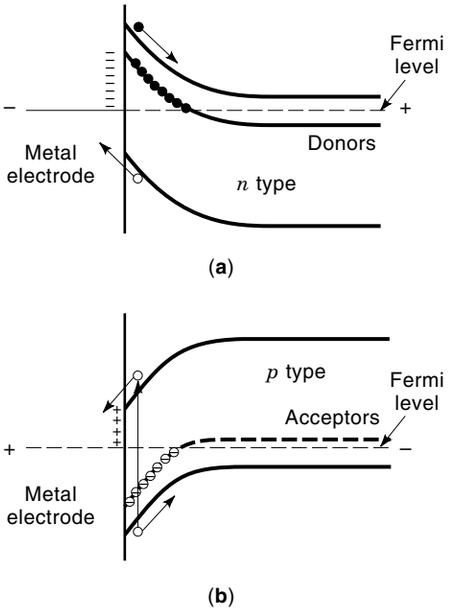

Figure 4. Energy-band diagrams for metal–semiconductor Schottky barriers on (a) *n*-type and (b) *p*-type material.

of the semiconductor. Typical energy-band diagrams are given in Fig. 4. If a thin metal film is used so that most of the light can penetrate into the semiconductor, a Schottky barrier can be used as a photoconducting device with maximum $G^* = 1$.

A typical *p*–*n* junction is shown in Fig. 5. Electrons excited in the *p*-type material, or holes excited in the *n*-type material, can diffuse to the depletion layer edges (if they are excited close enough to the junction to reach it before recombining, that is, if the distance from their point of origin to the junction is not large compared to their diffusion length). Once an electron or hole has been collected, however, it cannot be replaced, and the maximum $G^* = 1$. This behavior is quite similar to the homogeneous material case shown in Fig. 3(c), in which the *p*-type semiconductor plays the role of a nonohmic contact for electrons to the depletion region, and the *n*-type semiconductor plays the role of a nonohmic contact for holes to the depletion region.

Gains greater than unity can be obtained by using semiconductor junctions in a way that resembles the homogeneous case of Fig. 3(d), using band-shape localization of one carrier rather than imperfection capture. Figure 6 shows two possible structures: an *n*–*p*–*n* junction [Fig. 6(a)], in which pho-

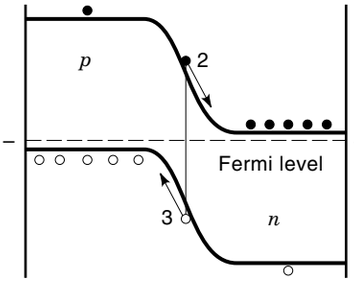

Figure 5. Energy-band diagram for a *p*–*n* junction.

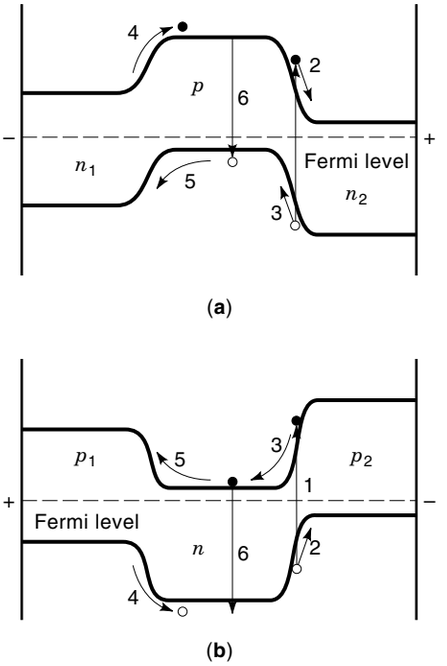

Figure 6. Energy-band diagrams for (a) an n–p–n junction and (b) a p–n–p junction.

toexcited holes are localized in the p region, allowing several transits of electrons across this region before the hole diffuses out or recombines, and an equivalent p–n–p junction [Fig. 6(b)], in which photoexcited electrons are localized in the n region, allowing several transits of holes across this region. The steps shown in Fig. 6(a), for example, are (1) photoexcitation of electron–hole pairs within a diffusion length of the p–n_2 junction, (2) collection of the photoexcited electron through n_2, (3) localization of the photoexcited hole in the p-type potential well formed by the junction structure, (4) injection of electrons from n_1 due to the extra positive charge of the hole, with continuing of this process until (5) the hole diffuses out of the p-type region or (6) the hole recombines with an electron. [This effect is analogous to that of a transistor with the holes, Fig. 6(a), supplied by light rather than a third external contact.] The gain is equal to the lifetime of the electrons passing through the p-type region, which is also equal to the time required for the holes to diffuse out of the p-type region [assuming step (5) is the dominant process], divided by the transit time of electrons across the p-type region by diffusion. The final expression for the gain is

$$G^* = (\sigma_{n1}/\sigma_p)(L_{pn}/W) \tag{11}$$

where $\sigma_{n1} = n_1 q\mu_n$, $\sigma_p = pq\mu_p$, L_{pn} is the diffusion length for holes in the n_1 material, and W is the width of the p-type region.

Polycrystalline Grain Boundaries

Related to these kind of effects are those encountered as the result of grain boundaries in a polycrystalline material. Figure 7 shows an energy-band diagram of an intergrain barrier in an n-type polycrystalline material. The structure resembles

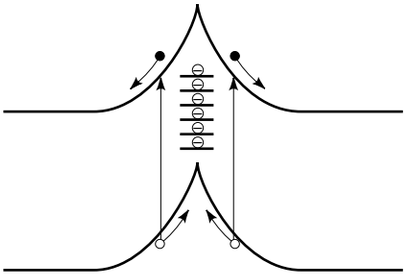

Figure 7. Energy-band diagram for an intergrain barrier in an n-type polycrystalline material.

that which would be expected for back-to-back Schottky barriers on the n-type material. If a voltage ΔV is applied to the grain boundary, such that the right-hand side in Fig. 7 is positive, then the effective barrier height on the right is increased from qV_b to $qV_b + q\Delta V$, and the effective barrier height on the left is decreased from qV_b to $qV_b - q\Delta V$. The result is that the flow of electrons to the right is larger than the flow of electrons to the left. The effective mobility μ^* in the material in the dark is proportional to $\exp(-qV_b/kT)$, and the effect of photoexcitation is to produce a change in conductivity through a change in both free-electron density Δn and a change in effective electron mobility, $\Delta\mu^*$, through a decrease in barrier height. The effects of photoexcitation in this case can be summarized as

$$\Delta\sigma = q\mu^*(1 + B)\,\Delta n \tag{12}$$

where $B = (\Delta\mu^*/\mu^*)/(\Delta n/n_0)$.

EXAMPLES OF RECOMBINATION MODELS

We summarize here three typical photoconductivity models suitable for describing many experimentally observed phenomena.

Shockley–Read Model

A model characterized by intrinsic photoexcitation, a single type of recombination center with capture coefficients β_n and β_p, and with thermal excitation processes between the center and both the conduction and valence bands, represents a classical example of a simple recombination situation (2). The same approach can be applied to the case of a number of different recombination centers.

The corresponding energy-band diagram is given in Fig. 8. Under a photogeneration rate G across the band gap, a free-

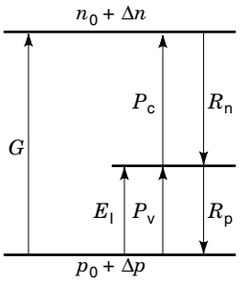

Figure 8. Energy-band diagram for the Shockley–Read recombination model. A recombination center with density N_l, characterized by capture coefficients β_n and β_p, lies E_l above the valence band.

electron density $n = n_0 + \Delta n$ and a free-hole density $p = p_0 + \Delta p$ exist. Electrons are captured by the imperfections with a rate R_n and holes with a rate R_p. Thermal excitation of electrons out of the imperfection to the conduction band and of holes out of the imperfection to the valence band are included in the model. In steady state $G = R_n = R_p$, $\tau_n = \Delta n/G$, and $\tau_p = \Delta p/G$. The general mathematical solution in algebraic form is relatively complex and depends for its detailed form on the relative magnitudes of Δn and Δp compared to n_0 and p_0, and on whether electrons and holes have equal or different lifetimes.

Large-Signal Computer Model

A model can be defined for a simple computer solution, based on the Shockley–Read approach, including a number of different imperfection levels, both capture and thermal processes, and valid when $\Delta n \geq n_0$. The model includes three types of relations.

1. Carrier conservation, so that for every electron-occupied state under photoexcitation that was empty in the dark there is a hole-occupied state under photoexcitation that was filled in the dark:

$$n - n_0 + \sum_i (n_i - n_{i0}) = p - p_0 + \sum_j [(N_j - n_j) - (N_j - n_{j0})] \tag{13}$$

   The sum on the left of Eq. (13) is taken over all levels with $E_i - E_v > E_{F0} - E_v$, and the sum on the right is taken over all levels with $E_j - E_v < E_{F0} - E_v$, where E_{F0} is the equilibrium Fermi energy. Values of the densities n_0, p_0, n_{i0}, and n_{j0} are calculated from the location of the Fermi energy as usual.

2. Continuity equations for electrons or holes. The continuity equation for holes, for example, is given by

$$G = \sum_i n_i \beta_{ip} p - \sum_j (N_j - n_j) P_{jv} + \beta_{cv}\, n\, p \tag{14}$$

   where G is the photoexcitation rate, β_{ip} is the capture coefficient for imperfections i with occupied density n_i for free holes with density p, P_{jv} is defined as $P_{jv} = N_v \beta_{jp} \exp[-(E_j - E_v)/kT]$, where N_v is the effective density of states in the valence band, $(N_j - n_j)P_{jv}$ is the thermal rate of emptying of holes from imperfections j to the valence band, and β_{cv} is the capture coefficient for free electrons by free holes.

3. A set of continuity equations for the electron occupancy of each of the imperfections, giving for each imperfection i the following equation:

$$n_i/N_i = (\beta_{in} n + P_{iv})/(\beta_{in} n + \beta_{ip} p + P_{ic} + P_{iv}) \tag{15}$$

   where $P_{ic} = N_c \beta_{in} \exp[-(E_G - E_i)/kT]$, where N_c is the effective density of states in the conduction band and nP_{ic} is the thermal rate of emptying of electrons from imperfections i to the conduction band.

The equivalency of a general solution of the Shockley–Read equation and the solution of this computer-formulated problem are shown by the results of Fig. 9.

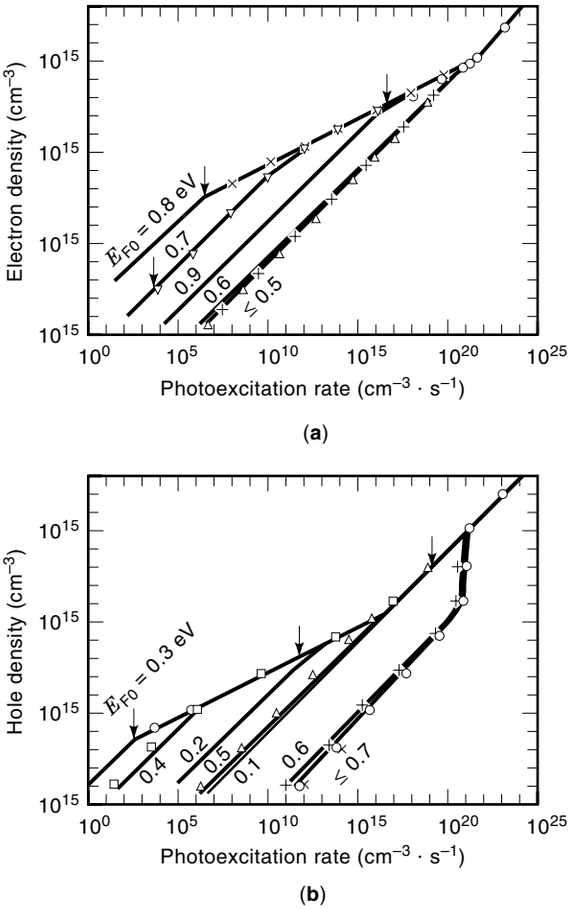

Figure 9. Comparison of (a) electron density and (b) hole density as calculated from the formal solution of the Shockley-Read equation (solid curves) and those calculated from the computer model (data points) for different values of Fermi energy, E_{F0}, for acceptors with $N_A = 10^{15}$ cm^{-3}, $E_A = 0.6$ eV, $E_G = 1.0$ eV, $\beta_n = 10^{-16} v_n$ cm$^3 \cdot$ s^{-1}, $\beta_p = 10^{-12}(300/T)^2\, v_p$ cm$^3 \cdot$ s^{-1} at 100 K, $\beta_{cv} = 10^{-20}(v_n v_p)^{1/2}$, $m_e^* = 0.2m$, and $m_h^* = 0.5m$. Arrows indicate in (a) the points at which $n = n_0$ for $E_{F0} = 0.7$ eV, 0.8 eV, and 0.9 eV, and in (b) the points at which $p = p_0$ for $E_{F0} = 0.1$ eV, 0.2 eV, and 0.3 eV.

Multivalent Imperfection Models

The dangling-bond imperfection in hydrogenated amorphous silicon (a-Si : H) is a multivalent imperfection with three energy states (not just full and empty as in the previous cases): a negatively charged state, D^-, occupied by two electrons; a neutral state, D^0, occupied by one electron, which can give rise to paramagnetic effects; and a positively charged state, D^+, electron unoccupied. Such imperfections can be formed in a variety of ways, including response to photoexcitation itself, giving rise to the description *optical degradation* for the decrease in free-carrier lifetime observed with increasing time of photoexcitation. A representative energy-band diagram for this case is shown in Fig. 10 for one kind of multivalent defect. In the more general case there may be several different multivalent defects, and the assumption of two different multivalent effects appears to give the best simple correlation with experimental data on photoconductivity versus the dark Fermi energy and photoconductivity as a function of imperfec-

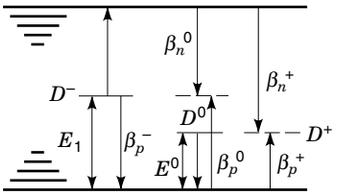

Figure 10. Model for photoconductivity in a material with trivalent imperfections, as for dangling-bond defects in hydrogenated amorphous silicon (a-Si : H), with states D^-, D^0, and D^+, showing also the recombination coefficients β and the various transitions included in the model. Also included are an exponential distribution of conduction- and valence-edge tail states. Unoccupied energy levels are shown as dashed lines.

tion density. Use of the model follows the computer model example given previously, and five steady-state equations are used in order to solve for the five unknowns, n, p, $[D^-]$, $[D^0]$, and $[D^+]$, where the square brackets indicate "density of."

RECOMBINATION EFFECTS FOR TWO TYPES OF IMPERFECTIONS

A number of phenomena of interest occur when there are at least two different types of imperfections, particularly when these have markedly different capture coefficients. A typical case is for two imperfections with large differences in electron-capture coefficients; imperfections with a large capture coefficient for electrons are called *recombination centers,* and imperfections with a small capture coefficient for electrons are called *sensitizing centers.* Measurements on the capture cross section of sensitizing centers in a variety of materials such as CdS, CdSe, GaAs, InP, ZnS, Ge, and Si indicate that the electron-capture cross section of a sensitizing center is usually of the order of 10^{-20} cm^2 to 10^{-22} cm^2. A representative energy-band diagram for this situation is given in Fig. 11. The most often-encountered phenomena can be described briefly as follows, using electrons as the majority carriers for simplicity.

Imperfection Sensitization

Under appropriate circumstances the incorporation of additional imperfections in a material actually causes the lifetime

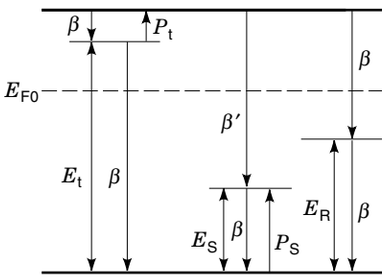

Figure 11. Energy-band diagram for a simple two-center recombination model with sensitizing centers lying E_S above the valence band, recombination centers lying E_R above the valence band, and electron traps lying E_t above the valence band. To simplify the notation all recombination coefficients are assumed equal to β, except for the electronic capture by sensitizing imperfections for which $\beta' \ll \beta$.

of electrons to be increased, thereby making the material a more sensitive photoconductor. If the imperfections introduced (e.g., doubly negative Cd vacancies formed to compensate the donors in CdS upon incorporation of a Cl impurity) have a small capture cross section for electrons and a large capture cross section for holes, as would be expected if the imperfections were doubly negatively charged, these imperfections will effectively become singly negative under photoexcitation through hole capture, and the corresponding electrons will become long-lived free electrons facing a Coulomb-repulsive barrier to capture at the imperfections.

Thermal Quenching of Photoconductivity

One characteristic of the photoconductivity in a material with two-center effects is an abrupt decrease in photoconductivity with increasing temperature, called *thermal quenching,* as shown in Fig. 12(a). When holes are no longer thermally stable at sensitizing centers, they are released and move to imperfections where the capture of an electron is more likely, thus removing the imperfection sensitization effect.

Superlinear Photoconductivity

Figure 12(b) shows the same data as Fig. 12(a), but plotted as photocurrent versus light intensity at constant temperatures. A natural consequence of the existence of thermal quenching in Fig. 12(a) is the existence of ranges of superlinear photoconductivity ($\Delta\sigma \propto G^\gamma$ with $\gamma > 1$) in Fig. 12(b). Over the superlinear range, increasing light intensity acts to overcome the effects of the thermal release of captured holes from sensitizing centers, and so at a fixed temperature the material becomes more sensitive with increasing light intensity.

Optical Quenching of Photoconductivity

Holes localized at sensitizing centers to produce a high electron lifetime may be freed, not only by thermal effects at higher temperature, but by irradiation with a second light source capable of optically exciting these holes to the valence band, with similar consequences for the electron lifetime. The time dependence of photocurrent for different photon energies of this second light source are shown in Fig. 13. At the shorter wavelengths, photoexcitation by the secondary light dominates over its quenching effect, whereas for longer wavelengths the quenching effect finally dominates. A plot of the magnitude of the quenching effect as a function of the wavelength of the second light source gives rise to an optical quenching spectrum.

Negative Photoconductivity

A much less frequently observed phenomenon is an actual decrease in photoconductivity from the dark value by irradiation with light. A possible model involves the existence of a sensitizing center lying above the Fermi level. Photoexcitation raises an electron from the valence band to this empty sensitizing center. The photoexcited hole is captured by a recombination center, which then removes an electron from the conduction band by recombination before the electron in the sensitizing level is thermally excited to the conduction band. Effectively the free electron is removed from the conduction band and localized on the sensitizing imperfection that was empty in the dark. For typical electron-capture coefficients for

recombination and sensitizing centers, a look at the competing processes indicates that this effect requires that the energy level for the sensitizing center lie less than about 0.3 eV above the Fermi level.

Saturation of Photoconductivity

If the photoexcitation intensity on a photoconductor containing sensitizing imperfections is increased to high values, it is found that the photoconductivity as a function of intensity effectively saturates. Saturation of the photoconductivity occurs when the photoexcitation rate is sufficiently high that essentially all of the sensitizing imperfections are hole-occupied. Then increasing the photoexcitation rate produces free electrons with corresponding holes, not at sensitizing centers, but at recombination centers with a much higher capture coefficient. The density of sensitizing imperfections is given by the sum of the saturated free-electron density and the corresponding density of photoexcited trapped electrons.

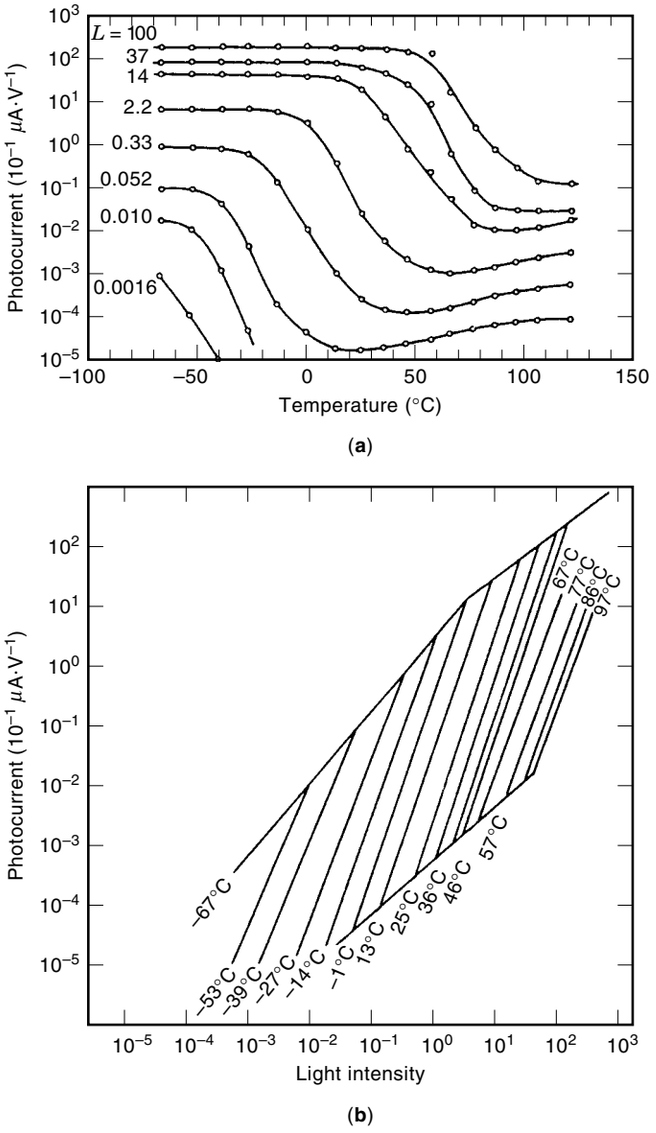

Figure 12. (a) Photocurrent for a CdSe crystal as a function of temperature for different photoexcitation intensities, and (b) the same data plotted as photocurrent as a function of photoexcitation intensity for different temperatures.

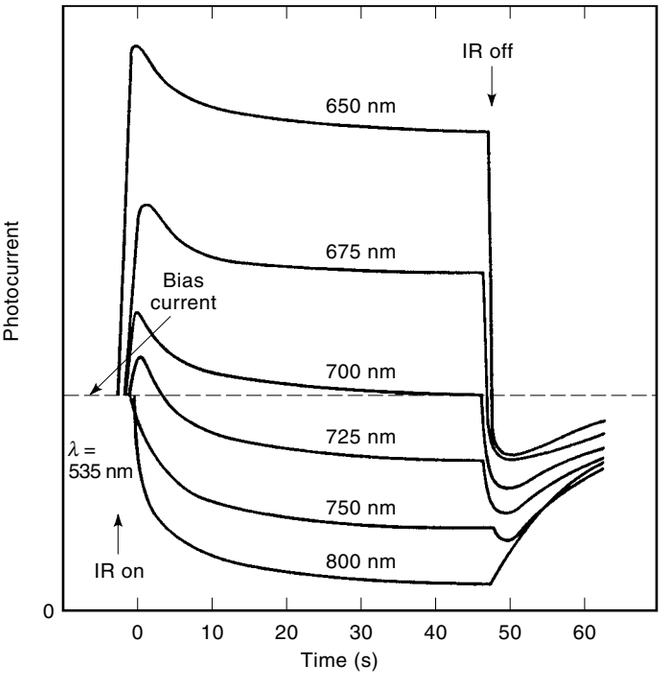

Figure 13. Optical quenching of photoconductivity shown here as the variation of photocurrent in CdS with time during photoexcitation by a primary infrared (IR) light source with wavelength of 535 nm, and secondary light sources with wavelengths between 650 nm and 800 nm.

Illustration of a Sensitizing Center: Zinc Impurity in Silicon

The case of a Zn impurity in silicon single crystals is a simple illustration of these sensitizing center effects for which the identity and properties of the sensitizing imperfections are known. The Zn impurity in Si has a single acceptor level Zn′ lying 0.31 eV above the valence band and a double acceptor level Zn″ lying 0.57 eV above the valence band at room temperature. When the Fermi level lies above the double-acceptor level, most of the Zn is in the Zn″ state and behaves like sensitizing imperfections for n-type photoconductivity. At 80 K the photoconductivity shows an optical quenching spectrum with a low-energy threshold of 0.58 eV, the energy required to excite an electron from the valence band to the Zn′ level to form a Zn″ center. The photoexcited electron density (measured by the photo-Hall effect) shows saturation with increasing excitation intensity. At low temperatures the charge of the Zn impurities is changed from -2 to -1 as the result of hole capture, which yields an increase in electron mobility due to a decrease in charged impurity scattering. Measurement of the electron-capture cross section of Zn′ imperfections from the onset of optical quenching of photoconductivity gives a value of 10^{-20} cm^2 at low temperatures.

RECOMBINATION PROCESSES

When a photoexcited electron is captured by a hole, there are three fundamental processes by which the energy given up by

the electron can be dissipated: (1) emitting photons—a radiative recombination, commonly called luminescence; (2) emitting phonons, either simultaneously or sequentially, a nonradiative process; or (3) raising other free carriers, either electrons or holes, to higher energies in their bands, another nonradiative process called Auger recombination, after which the carriers may relax by the emission of phonons.

Radiative Recombination

Radiative recombination may be the process involved in the recombination of a free electron and a free hole with the emission of a photon. The probability for this process to be radiative is higher in materials with direct rather than indirect band gaps. The optically stimulated emission of radiation by the electrical injection of free carriers gives rise to the phenomena associated with solid-state lasers. A typical cross section for radiative capture by a neutral or Coulomb-repulsive imperfection is about 10^{-19} cm^2 at 300 K.

A simple schematic summary of three main ways of achieving radiative recombination involving imperfections is given in Fig. 14: (1) recombination between a free carrier and a localized carrier; (2) recombination of two localized carriers on imperfections sufficiently close in space such that the wave functions of the localized electron and hole overlap, which is often called a *pair transition* and for which the peak emission energy shifts with photoexcitation intensity and time during decay; and (3) recombination between the excited state and the ground state of an impurity in a semiconductor with incompletely filled atomic levels; a typical impurity is Mn (incomplete d shell) that behaves as a luminescence center in many different semiconductors.

Phonon Emission

For radiative recombination, an electron energy of 1 eV can be dissipated by the emission of a single photon. But in nonradiative recombination through the emission of phonons, a total energy of 1 eV corresponds to about 20 to 30 phonons. If these phonons must be emitted simultaneously, the probability is relatively small. A typical cross section for nonradiative capture with the release of simultaneous phonons for a neutral recombination center is about $\leq 10^{-16}$ cm^2.

If the imperfection has a Coulomb attraction for the free electron, however, this transition probability can become much larger if the electron energy is dissipated by the cascade emission of phonons sequentially after the electron is initially captured in an excited state of the imperfection and then drops down step by step through the excited states of the imperfection, omitting just one or a few phonons at each step. A typical cross section for nonradiative capture with the release of sequential phonons for a Coulomb attractive recombination center is about 10^{-12} cm^2.

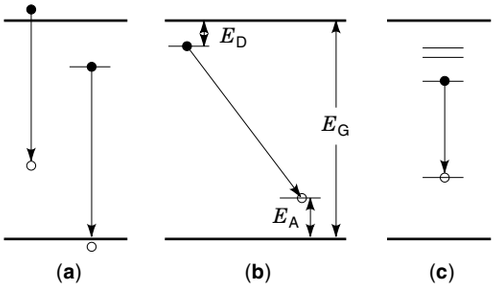

Figure 14. Three major types of radiative recombination: (a) recombination between a free carrier and a localized carrier, (b) pair recombination between a nearby donor and acceptor, and (c) recombination between the atomic levels of an impurity ion.

Another dramatic multiphonon recombination process has been described for specific deep imperfection states in semiconductors, in which nonradiative capture of an electron is accompanied by the emission of many local phonons corresponding to a major change in the configuration of the imperfection and the position of its energy level before and after capture. For the case of a particular defect in n-type GaAs, the electron-capture cross section varied from less than 10^{-20} cm^2 at 200 K to 10^{-18} cm^2 at 400 K (3).

If the imperfection has a Coulomb repulsion for the free electron, capture of the electron requires either thermal excitation over the potential barrier surrounding the imperfection or tunneling through this barrier. The small values of capture cross section for sensitizing centers, cited previously, arise from this type of interaction. A typical cross section for nonradiative capture with the release of sequential phonons for a Coulomb repulsive recombination center is about $\leq 10^{-19}$ cm^2.

Auger Recombination

In an Auger recombination process, the excess energy of the recombining electron is given to another free carrier, most likely a majority carrier since the probability for energy transfer in this way is proportional to the density of the other free carriers. The Auger process is the inverse of impact ionization, in which a high-energy free carrier gives up its energy to a bound carrier to raise it to the band. The rate of Auger-controlled recombination for electrons in an n-type semiconductor with N_I recombination imperfections can be expressed as

$$(\text{Rate}) = n(Bn)(N_I - n_I) \tag{16}$$

The capture coefficient for nonradiative capture by an Auger process for a neutral or Coulomb repulsive recombination center is of the form $\beta_n = Bn$. A typical value for the Auger coefficient B can be obtained by mathematically balancing impact ionization with Auger recombination for a hydrogenlike center, giving a value of B of about 10^{-24} cm$^6 \cdot$ s^{-1} (4). The magnitude for this parameter B in cases in which nonhydrogenic imperfections are involved has been tested by measuring optical quenching breakpoints as a function of the quenching light intensity; in the case of GaAs crystals, for example, results indicate that $B < 10^{-28}$ cm$^6 \cdot$ s^{-1} (5).

STEADY-STATE PHOTOELECTRONIC ANALYSIS

Measurements of photoconductivity-related phenomena are often useful in obtaining information about the electronically significant properties of a material. A brief summary of some of the techniques and their results are given here to indicate the nature of these applications. In this section we consider some of the steady-state techniques, and in the following section some of the transient techniques.

Optical Absorption

Spectral response curves for the absorption constant α are a standard technique for measuring the energies of imperfection energy levels in a semiconductor by determining the minimum energy required to excite a carrier from an imperfection to a band. Practical problems are involved in the attempt to measure small absorption constants in thin-film materials. One solution is to substitute photoconductivity spectral response for optical absorption spectral response. The use of ac techniques which reduce the effects of noise for the photoconductivity allows amplification to make even a small signal measurable. In order to avoid spurious effects due to a variation of electron lifetime with the position of the Fermi level, the measurement is usually carried out by measuring the light intensity required to maintain constant photocurrent conditions and is known therefore as the constant photoconductivity measurement or CPM.

Steady-State Photoconductivity

As indicated in Eq. (2), the magnitude of the steady-state photoconductivity is proportional to the free-carrier lifetime and therefore provides a means of determining that lifetime.

Measurement of the photoconductivity as a function of photoexcitation rate G to determine the value of γ in $\Delta n \propto G^{\gamma}$ provides information useful for checking a photoconductivity model involving one or more traps and one or more recombination centers.

In a semiconductor containing sensitizing imperfections, measurements of breakpoints in superlinear behavior and thermal quenching as a function of photoexcitation intensity and temperature make possible determination of the hole ionization energy of the sensitizing centers and the ratio of their capture cross sections. Measurement of saturation of photoconductivity allows determination of the density of sensitizing centers. Optical quenching spectra provide additional information about the location of the imperfection energy level and the value of its majority-carrier capture cross section.

Minority-Carrier Lifetime

Consider the case shown in Fig. 3(d). If the applied voltage is large enough to sweep the photoexcited hole out of the sample before it can be captured at an imperfection, the photoconductivity saturates. If $\mathscr{E}_c$ is the critical electric field for saturation, $\tau_p \mu_p = d/\mathscr{E}_c$, where the approximate width of the sample is $2d$.

The photomagnetoelectric effect (PME) is the Hall effect of carriers diffusing away from a surface where they have been created by strongly absorbed light. The PME current is proportional to $\tau_{\min}^{1/2}$, where $\tau_{\min}$ is the minority-carrier lifetime. Information about the importance of surface recombination effects can be obtained by measuring the dependence of the PME current on magnetic field.

The measurement of the surface photovoltage caused by the absorption of light at a semiconductor surface enables measurement of the minority-carrier diffusion length, and hence the minority-carrier lifetime. A photovoltage is developed between the surface and the bulk due to the back diffusion of minority carriers to the surface barrier and the subsequent charge separation of the hole–electron pairs in the barrier field (6). Experimentally the surface photovoltage is kept constant by varying the photon flux; a plot of photon flux versus $1/\alpha(\lambda)$ produces a straight line with intercept on the negative $1/\alpha(\lambda)$ axis of $L_{\min}$.

Electron- and photon-beam-induced currents can be used to determine the minority-carrier diffusion length $L_{\min}$ by scanning a small region of the material with an electron-beam induced current (EBIC) or a light beam as a function of distance x from a junction involving the material. For reasonably large values of $x/L_{\min}$, the induced current is proportional to $\exp(-x/L_{\min})$.

A technique known as the *steady-state photocarrier grating technique* makes it possible to measure the ambipolar diffusion length under steady-state conditions in insulating photoconductive materials (7). Interference between two coherent light beams with different intensities is achieved, in order to create a grating superposed on a uniformly illuminated background. If the grating spacing is much larger than the diffusion length, a well-defined photocarrier grating is created, but if the grating spacing is much less than the diffusion length, an effectively uniform photocarrier distribution results. Measurement of the photocurrent perpendicular to the grating fringes as a function of the grating period permits determination of the diffusion length.

Phototransport Effects

A number of techniques useful for measuring electronic properties of semiconductors in the dark may be broadened to application to situations in which the material is under photoexcitation.

The photo-Hall effect can be used to separate the effects of photoexcitation on carrier density and mobility and to detect changes in majority-carrier type as a function of photoexcitation intensity and/or temperature.

Similar results may be obtained from the photothermoelectric effect, which also separates carrier density and mobility effects under photoexcitation due to the presence of a thermal gradient in the material.

The capacitance of a semiconductor junction changes under photoexcitation due to a change in the charge in the depletion region of the junction. The sign and the magnitude of the capacitance change as a result of photoexcitation can be used to obtain information about the charge state and density of the imperfection levels in the depletion layer. Measurements of the initial time dependence of the capacitance upon start of photoexcitation can be used to determine values for the optical cross section of a particular set of imperfections as a function of photon energy if their density is known. The spectral response of optical quenching of thermally stable photoinduced capacitance at low temperatures can also be used to indicate the location of imperfection levels.

Near-View Photoconductivity

A technique known as near-view photoconductivity (NPC), related to near-field scanning optical microscopy (NSOM), has been developed to enable the characterization of defects at a submicron length scale, which gives higher resolution than electron-beam induced conductivity (EBIC). The NPC technique represents a near-imaging method using the super-resolution of NSOM. An image is generated in NSOM in which the near-field radiation is used to excite photoconductivity. The results show at least five times better resolution than

conventional photoconductivity or EBIC imaging. The NPC image gives a map of minority carrier transport with a resolution of about 250 nm. The technique is applicable to a wide variety of electronic and optoelectronic materials such as transistors, light-emitting diodes, photodectors, and lasers, giving the ability to understand transport properties on an nm scale (8,9).

TRANSIENT PHOTOELECTRONIC ANALYSIS

Decay Transients

Transient methods of photoelectronic analysis focus on the rise or decay of photoinduced imperfection occupancies. These methods can be applied to photoconductivity and photocapacitance. From measurements of their variation with time, one can deduce values for the ionization energy, optical cross section, capture cross sections, and density of the imperfection involved. Similar insights can be obtained from measurements of the decay of luminescence.

Two extreme cases in decay yield to simple interpretation: (1) the case of no retrapping, so that a carrier thermally freed from a trap during decay recombines before being retrapped, in which case the decay curve is a simple exponential; and (2) the case of strong retrapping, so that an effective balance exists between carriers being thermally freed from traps and free carriers being trapped, in which case the steady-state Fermi level can be used to indicate trap occupancy and it is possible to deduce the density distribution of trapped carriers versus depth from the decay curves.

A decay-sampling technique particularly suited to computerized analysis is known as the *rate window* approach. Two times are chosen during the decay process, t_1 and t_2 ($t_2 > t_1$), and the signal $Z(t)$ at each of these times is measured. Then $Z(t_1) - Z(t_2)$ is plotted as a function of temperature. For low temperatures, the decay is very slow and $Z(t_1) - Z(t_2)$ is small, and for high temperatures, the decay is very fast and completed before $t = t_1$, so that again $Z(t_1) - Z(t_2)$ is small. The result is a curve exhibiting a maximum at a particular temperature, which can be suitably interpreted to obtain the trap parameters. This general technique has been developed into what is frequently called photoinduced transient spectroscopy (PITS) or optical transient current spectroscopy (OTCS) (10).

Thermally Stimulated Measurements

Measurements of thermally stimulated decay are often used in which a certain distribution of imperfection occupancies is caused by photoexcitation at low temperature, and then the effect of releasing these trapped carriers is observed as a function of time as the sample is heated at a linear rate in the dark. Here we include thermally stimulated conductivity (TSC), thermally stimulated luminescence (glow curves), and thermally stimulated capacitance. Since it is possible to obtain the advantages of a Hall-effect measurement during thermal stimulation, it is appropriate also to speak about thermally stimulated Hall-effect measurements.

Quite similar to the rate window approach described previously, the TSC for a particular trapping imperfection is very small at low temperatures and at high temperatures, and exhibits a maximum in between. Depending on the analytical assumptions made, this TSC curve can be used to obtain information about the trap depth from the temperature at which maximum conductivity is observed and about the trap density from the area under the TSC curve.

QUANTUM WELLS AND SUPERLATTICES

New capabilities for shaping the properties of materials has come about in recent years made possible by the development of highly controllable deposition systems for thin films, such as molecular beam epitaxy (MBE) and organometallic chemical vapor deposition (OMCVD). These techniques have made it possible to deposit multilayer heterojunctions with atomically abrupt interfaces, and controlled compositions and doping, in individual layers that are only a few tens of nanometers thick. These layers are so thin that the energy levels in them in their small-dimension direction show the quantum effects predicted for an electron in a very narrow two-dimensional potential well.

If many quantum wells are grown on top of one another and the barriers are made so thin (<5 nm) that tunneling between them is significant, the result is a superlattice with properties controlled by the artificial periodicity of the multilayer structure (11). An example is shown in Fig. 15, where photoconductivity gains greater than unity are achievable by effects related to those of Figs. 3(d) and 6: localization of the photoexcited hole in superlattice wells, while photoexcited electrons are relatively free to move in a "miniband." Structures tested in this way consisted of an undoped $Al_{0.48}In_{0.52}As$(3.5 nm)/$Ga_{0.47}In_{0.53}As$(3.5 nm) 100 period superlattice sandwiched between two degenerately doped n^+, 0.45 μm thick, $Ga_{0.47}In_{0.53}As$ layers. For an applied voltage of 1.4 V, a gain of 2×10^4 was measured.

Other related possibilities of interest for photodetectors are devices utilizing sequential resonant tunneling in a superlattice, such as that shown in Fig. 16 (12). A bias voltage is chosen so that the second excited level in the nth well has the same energy as the third excited level in the $(n + 1)$th well. After tunneling, the electron can relax to the first excited state, whereupon it can again tunnel to the second excited state of the $(n + 2)$th well or it can relax to the ground state of the $(n + 1)$th well. A photocurrent results whenever the electron relaxes to the ground state in a different well from the one in which it was initially excited.

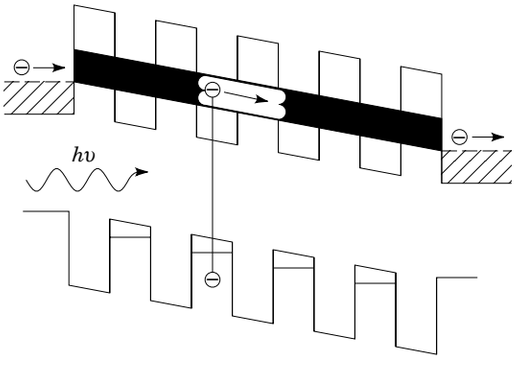

Figure 15. Band diagram of a superlattice photoconductor, showing effective localization of photoexcited holes in quantum wells, while electrons tunnel in a conduction miniband.

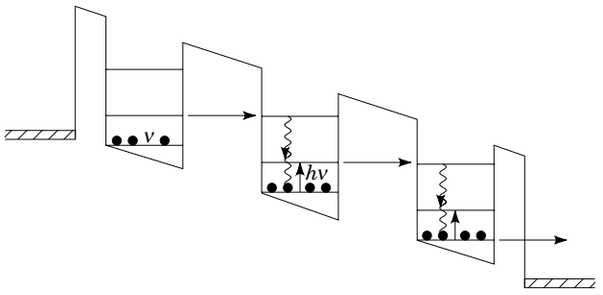

Figure 16. An infrared photoconducting detector utilizing sequential resonant tunneling.

Photodiodes with gain greater than unity can also be prepared making use of avalanche multiplication in special types of p–n junctions (11). In these devices, photoexcited carriers receive sufficient energy from the electric field to raise electrons from the valence band to the conduction band by impact ionization. Carriers produced by impact ionization take part in additional impact ionization excitation of carriers, resulting in an avalanche.

ACKNOWLEDGMENT

This article is based primarily on the material discussed in R. H. Bube, *Photoelectronic Properties of Semiconductors,* Copyright 1992 by Cambridge University Press, Cambridge, UK, which is the source for the figures that are used here, which are reprinted with the kind permission of Cambridge University Press. For additional detail, pertinent references etc., please see this book.

BIBLIOGRAPHY

1. R. H. Bube, *Photoelectronic Properties of Semiconductors,* Cambridge, UK: Cambridge Univ. Press, 1992.
2. W. Shockley and W. T. Read, *Phys. Rev.,* **87**: 835–842, 1952.
3. C. H. Henry and D. V. Lang, *Phys. Rev.,* **15**: 989–1016, 1975.
4. E. Burstein, *Photoconductivity Conference,* New York: Wiley, 1956, p. 353.
5. J. Saura and R. H. Bube, *J. Appl. Phys.,* **36**: 3660–3662, 1965.
6. A. R. Moore, in J. L. Pankove (ed.), *Semiconductors and Semimetals: Hydrogenated Amorphous Silicon,* Vol. 21C, New York: Academic Press, 1984, pp. 239–256.
7. D. Ritter, E. Zeldov, and K. Weiser, *Appl. Phys. Lett.,* **49**: 791–793, 1986.
8. S. K. Burato et al., *Appl. Phys. Lett.,* **65**: 2654–2656, 1994.
9. Q. Xu, M. H. Gray, and J. W. P. Hsu, *J. Appl. Phys.,* **82**: 748–755, 1997.
10. C. Hurtes et al., *Appl. Phys. Lett.,* **32**: 821–823, 1978.
11. F. Capasso, *Science,* **235**: 172–176, 1987.
12. F. Capasso, K. Mohammed, and A. Y. Cho, *IEEE J. Quant. Electron.,* **QE-22**: 1853–1869, 1986.

Reading List

R. H. Bube, *Photoconductivity of Solids,* New York: Wiley, 1960; Huntington, NY: Krieger, 1978.

R. H. Bube, Photoconductivity of Semiconductors, in H. Eyring, D. Henderson, and W. Jost (eds.), *Physical Chemistry,* Vol. X, *Solid State,* New York: Academic Press, 1970, p. 515.

F. Capasso (ed.), *Physics of Quantum Electron Devices,* New York: Springer-Verlag, 1990.

N. V. Joshi, *Photoconductivity: Art, Science and Technology,* New York: Dekker, 1990.

J. Mort and D. M. Pai (eds.), *Photoconductivity and Related Phenomena,* New York: Elsevier, 1976.

T. S. Moss, *Photoconductivity in the Elements,* New York: Academic Press, 1952.

A. Rose, *Concepts in Photoconductivity and Allied Problems,* New York: Wiley Interscience, 1963.

S. M. Ryvkin, *Photoelectric Effects in Semiconductors,* New York: Consultants Bureau, 1964.

RICHARD H. BUBE
Stanford University

PHOTOCURRENT. See PHOTOVOLTAIC EFFECTS.